Efficient Representation of Topologically Ordered States with Restricted Boltzmann Machines

Sirui Lu,[1,2] X. Gao,[2,3,*] and L.-M. Duan[2,†]

[1] *Department of Physics, Tsinghua University, Beijing 100084, China*
[2] *Center for Quantum Information, Institute for Interdisciplinary Information Sciences, Tsinghua University, Beijing 100084, China*
[3] *Department of Physics, Harvard University, Cambridge, MA 02138, USA*

(Dated: May 13, 2019)

Representation by neural networks, in particular by restricted Boltzmann machines (RBM), has provided a powerful computational tool to solve quantum many-body problems. An important open question is how to characterize which class of quantum states can be efficiently represented with the RBM. Here, we show that the RBM can efficiently represent a wide class of many-body entangled states with rich exotic topological orders. This includes: (1) ground states of double semion and twisted quantum double models with intrinsic topological orders; (2) states of the AKLT model and 2D CZX model with symmetry protected topological order; (3) states of Haah code model with fracton topological order; (4) generalized stabilizer states and hypergraph states that are important for quantum information protocols. One twisted quantum double model state considered here harbors non-abelian anyon excitations. Our result shows that it is possible to study a variety of quantum models with exotic topological orders and rich physics using the RBM computational toolbox.

Introduction.—Deep learning[1, 2] has become a powerful tool for scientific discovery. Recently deep learning methods have attracted considerable attention in quantum physics[3, 4], especially for attacking quantum many-body problems. The difficulty of quantum many-body problems mainly originates from the exponential growth of the Hilbert space dimensions. To overcome this exponential difficulty, researchers traditionally use tensor network methods [5–7] and Quantum Monte Carlo(QMC) methods [8]. However, QMC methods suffer from the sign problem [9]; Tensor network methods cannot deal with high dimensional system [10] or massive entanglement [11]. The neural network, one of the fundamental building block of deep learning, has been recently employed as a compact representation of quantum many-body state[12–22]. Many variants of neural network have been investigated numerically or theoretically, such as restricted Boltzmann machines(RBM)[12, 13, 15, 21], deep Boltzmann machine(DBM) [15, 16, 22] and feed-forward Neural Network(FNN)[18]. We focus on RBM states which work efficiently during variational optimization although the representational power of which is somewhat limited [15]. The RBM ansatz also plays a role in quantum state tomography[23], classical simulation of quantum circuits[24], and the detection of Bell nonlocality[25].

In the past decades, the studies of topological order [26, 27] which are beyond the framework of Landau's symmetry breaking paradigm [28] have attracted tremendous attention. There are several types of topological orders; First, intrinsic topological order features unliftable ground state degeneracy by local perturbations. Second, it comes symmetry protected topological(SPT) order; SPT states with a given symmetry cannot be smoothly deformed into each other without a phase transition if the deformation preserves the symmetry. The third is the fracton topological order. The hallmark of fractons is their ability to harbor point excitations that are immobile in 3D space. While several studies have shown that RBM states can capture simple many-body states such as graph/cluster state [13, 15] and toric/surface code state [13, 15, 21], no single study exist which represents other more exotic topological states in the condensed matter physics [26, 27, 29, 30].

To fill this gap, we use tools from quantum information to construct RBM representations for other notable many-body states with different topological orders. Many of exotic condensed matter topological states can be described by powerful quantum information tools: (i) the hypergraph state formalism which is a generalization of the graph-state formalism; (ii) the stabilizer formalism [31] which describes most of the quantum error correction code; (iii) the XS-stabilizer formalism [32] which is a generalization of the stabilizer formalism. We prove these states of (i-iii) can be represented as RBM efficiently based on the properties of their wave function. To study higher spin systems, we propose a unary RBM representation.

These tools from quantum information provide recipes for constructing RBM representation within their formalism. The stabilizer formalism describes many fracton models [33–38] such as Haah's code [33]. Concerning the intrinsic topological order, we show RBM states can capture double semion of string-net model [39, 40] and many twisted quantum double model [41–43] using their XS-stabilizer description. For symmetry protected topological order, we give exact constructions of the AKLT model [44, 45] with unary representation. We also consider RBM representation for other SPT models such as

2D CZX model [46]. Our exact representation results are insightful for future studies of quantum topological phase transition and quantum information protocols.

RBM state.—We first recall the definition of RBM state, describe notations and introduce some useful identities. In the computational basis, a quantum wave function of n-qubit can be expressed as $|\Psi\rangle = \sum_{\mathbf{v}} \Psi(\mathbf{v})|\mathbf{v}\rangle$ with $\mathbf{v} \equiv (v_1, \ldots, v_n)$, where the $\Psi(\mathbf{v})$ is a complex function of n binary variables v_i. We use $\{0, 1\}$ valued vertices instead of $\{-1, 1\}$ valued vertices for convenience. In the case of RBM, $\Psi(\mathbf{v}) = \sum_{\mathbf{h}} e^{W(\mathbf{v},\mathbf{h})}$, where the weight $W(\mathbf{v}, \mathbf{h}) = \sum_{i,j} W_{ij} v_i h_j + \sum_i a_i v_i + \sum_j b_j h_j$ is a complex quadratic function of binary variables. While DBM allow arbitrary intra-layer connection, in RBM the visible neurons $\mathbf{v}$ only connect to hidden neurons $\mathbf{h}$. Let the number of visible neurons be n and the number of hidden neurons be m. We say the representation is efficient if $m = \text{ploy}(n)$. The whole wave function writes

$$\Psi_{\text{RBM}}(\mathbf{v}) = e^{\sum_{i=1}^{n} a_i v_i} \prod_{j=1}^{m} (1 + \exp(\theta_j)) \tag{1}$$

with effective angles $\theta_j = b_j + \sum_{k=1}^{n} W_{kj} v_k$.

The parity constraint is an important class of constraints that are easy to construct by RBM. A hidden neuron that connects to each of these visible neurons $v_1, v_2, \cdots, v_k$ with weight function $W(v, h) = i\pi v h - (\ln 2)/4$ realizes the parity constraint: $(v_1 + v_2 + \cdots + v_k) \mod 2 = 0$ (this can be generalized to affine function: both equals to 0 and 1 are allowed). The RBM representation of toric code [13, 15] uses the case of $k = 4$. We will need this property later for generalized stabilizer formalisms.

To study higher spin systems, we propose the unary representation. The idea of unary representation is best illustrated using an example, as depicted in Fig. 1. We use three neurons(qubits) to represent a spin-1: $|100\rangle \to |-1\rangle$, $|010\rangle \to |0\rangle$ and $|001\rangle \to |1\rangle$ by restricting these three neurons(qubits) to the subspace spanned by $|100\rangle$, $|010\rangle$ and $|001\rangle$. This can be done by using two hidden neurons (blue neurons in Fig. 1). We left the details of the derivation in the appendix. Our unary representation is simpler than multi-value neurons or encoded binary neurons in distinguishing and decoding basis states. We will use this unary representation to represent AKLT state later.

RBM states [47] have been shown to represent graph states efficiently [13, 15]. We recall the wave function of graph states takes the form $\Psi(v_1, \cdots, v_n) = \prod_{\{i,j\}} (-1)^{v_i v_j}$ (up to a normalization factor), where $\{i, j\}$ denotes an edge linking the i-th and j-th qubits represented by visible neurons v_i, v_j. If one hidden neuron h connects to two visible neurons v_i and v_j with weight $W_H(x_i, h) = \frac{\pi}{8} i - \frac{\ln 2}{2} - \frac{\pi}{2} i x - \frac{\pi}{4} i h + i\pi x h$, the correlation factor between v_i and v_j is $(-1)^{v_i v_j}$.

There are various ways to generalize graph states, as depicted in Fig. 2. Hypergraph states [48] generalize graph states by introducing more than two body correlation factor such as $(-1)^{v_1 v_2 v_3}$. Stabilizer states generalize graph states through additional local Clifford operations [49–51], which impose parity constraints and extra phases(we will show this later). XS-stabilizer states [32] combines 3-body correlation factors from hypergraph state and parity constraints from stabilizer states. We now proceed to prove these classes of states can be represented as RBM exactly and efficiently.

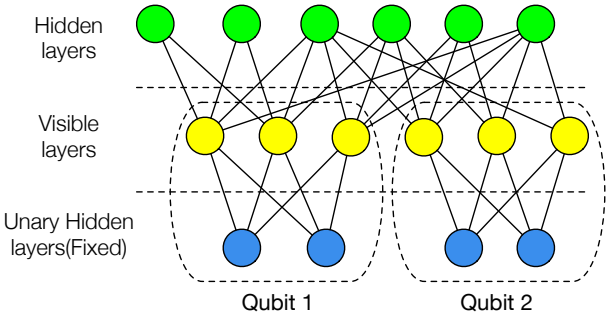

FIG. 1. The unary RBM representation for higher spin systems. The three left yellow neurons correspond to the qubit 1, and the three right yellow neurons correspond to the qubit 2. Two blue neurons in the unary hidden layers restrict three visible yellow neurons to be one of 001, 010 and 001 that corresponds to $|-1\rangle$, $|0\rangle$ and $|+1\rangle$ in spin-1. The whole graph is still a bipartite graph.

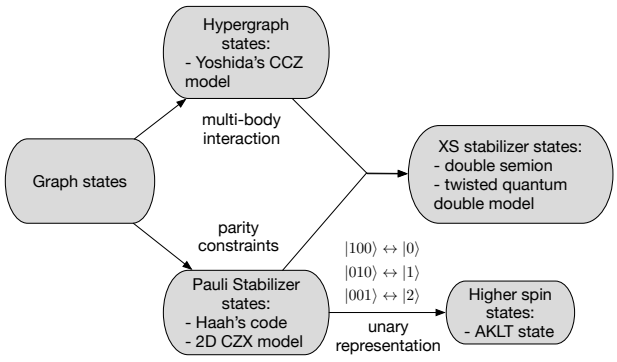

FIG. 2. Different generalizations of graph state. (a) Hypergraph states generalize graph states by introducing 3-body correlation factor; (b) Stabilizer states generalize graph states by additional parity constraints on qubits; (c) XS-stabilizer states combine the parity constraints from Pauli stabilizer and 3-body correlation factor from hypergraph state. Many condensed matter topological models fall into these quantum information formalisms, thus can be represented by RBM. We will encounter them later. Combining with unary representation, stabilizer state with added unary constraints can describe AKLT state. Thus AKLT state can be represented as RBM.

RBM representation of hypergraph states.— Hypergraphs generalize graphs by allowing an edge can join

any number of vertices. We define an edge that connects k vertices a k-hyperedge. Given a mathematical hypergraph, the wave functions of its corresponding hypergraph states [48] take the form:

$$\Psi_{\text{hypergraph}}(\mathbf{v}) \propto \prod_{\{v_1,v_2,\ldots,v_k\}\in E} (-1)^{v_1 v_2 \ldots v_k}.$$

The notation $\{v_1, v_2 \ldots, v_k\} \in E$ means that these k vertices $\{v_1, v_2 \ldots, v_k\}$ are connected by a k-hyperedge. We illustrate the correspondence in Fig. 3. In this work, we extend RBM representation to hypergraph states.

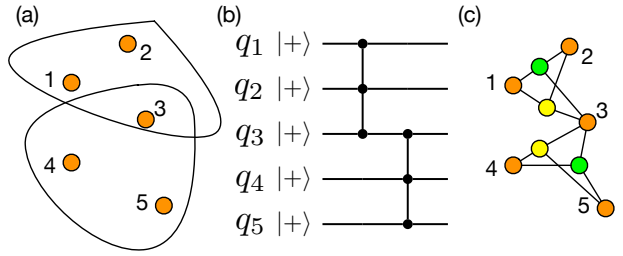

FIG. 3. RBM representation of hypergraph state. (a) A hypergraph. There are two 3-hyperedges that connect $\{q_1, q_2, q_3\}$ and $\{q_3, q_4, q_5\}$. (b) The encoding circuit of this hypergraph state. (c) The corresponding RBM representation of (a). Orange neurons are visible neurons, and both green and yellow vertice are hidden neurons. The two different colors(yellow and green) resemble different weight functions.

Theorem 1 *Restricted Boltzmann machines can represent any hypergraph states efficiently.*

In the main text, we take the graph with 3-hyperedges as an example, which will be useful later for XS-stabilizer state and one SPT state. Precisely we obtained the following decomposition:

$$(-1)^{v_1 v_2 v_3} = e^{i\pi(\sum_{i=1}^3 v_i)} \cdot \sum_{h_1,h_2} e^{w(\sum_{i=1}^3 v_i)(h_1-h_2)+b(h_1+h_2)+c}, \tag{2}$$

where $w = i$, $b = \ln(\frac{1+\sqrt{-15}}{4})$ and $c = \ln\frac{2}{3} - b$. Thus, the exact RBM representation of $(-1)^{v_1 v_2 v_3}$ makes use of two hidden neurons, as shown in Fig. 3 (c). The method for decomposing $(-1)^{v_1 v_2 v_3}$ can be extended to treat $(-1)^{v_1 v_2 \cdots v_k}$ for arbitrary k with $2k + O(1)$ hidden neurons. We leave the details of the derivation and the proof in the appendix.

RBM representation of XS/Paui-stabilizer state.— The Pauli stabilizer formalism generalizes graph states by applying some local Clifford transformations [50, 52]. The XS-stabilizer formalism generalizes the Pauli stabilizer formalism [32] by changing the single qubit Pauli group to Pauli-S group $\mathcal{P}^S = \langle \alpha I, X, S\rangle$ where $\alpha = \mathrm{e}^{\mathrm{i}\pi/4}$ and $S = \mathrm{diag}(1, \mathrm{i})$. This group contains the Pauli group since $S^2 = Z$.

Theorem 2 *Restricted Boltzmann machines can represent any Pauli-stabilizer states and XS-stabilizer states efficiently.*

Our proof is based on the wave function of the stabilizer state first proved in [49, 53] and the similar result on XS-stabilizer state proved in [32]. Let $\delta(x)$ satisfies $\delta(0) = 1$ and $\delta(1) = 0$. The wave functions of every Pauli-stabilizer state and XS-stabilizer state on n qubits can be written as the closed form of

$$\Psi_{\text{pauli}}(\mathbf{v}) \propto i^{l(\mathbf{v})}(-1)^{q(\mathbf{v})} \prod_j \delta(L_j^p \bmod 2) \tag{3}$$

$$\Psi_{\text{XS}}(\mathbf{v}) \propto \alpha^{l(\mathbf{v})} i^{q(\mathbf{v})}(-1)^{c(\mathbf{v})} \prod_j \delta(L_j^p \bmod 2) \tag{4}$$

where $l(\mathbf{v})$, $q(\mathbf{v})$ and $c(\mathbf{v})$ are linear, quadratic and cubic polynomials of $\mathbf{v}$ with integer coefficients respectively. The L_j^p are affine(linear terms plus constant term) functions of some subsets of $\mathbf{v}$. Moreover, these polynomials $l(x)$, $q(x)$ and $c(x)$ along with L_j^p can be determined efficiently from the given stabilizers.

Given this wave function, we can easily deduce its RBM representation: First, the $\prod_j \delta(L_j^p \bmod 2)$ parts correspond to parity constraints, which RBM can represent. Meanwhile, functions that are products of $i^{l(\mathbf{v})}$, $(-1)^{q(\mathbf{v})}$, $\alpha^{l(\mathbf{v})}$, $i^{q(\mathbf{v})}$ and $(-1)^{c(\mathbf{v})}$ can also be represented by RBM using techniques used for graph states and hypergraph states.

In the case of stabilizer states, we provide a new proof of the closed form wave function. First, a stabilizer state can be generated from a Clifford circuit [31] consisting of H, S, and CZ gates. From the encoding circuit, the stabilizer state can be represented by a DBM in the closed form directly. Then we can iteratively reduce it to an RBM while still keep the closed form. We left the details of the proof in the appendix.

We can make use of local Clifford equivalence between stabilizer state and graph states [50, 54] to further simplify our procedure. In fact, every stabilizer state can be chosen to be locally equivalent to a graph state such that only at most a single H or S gate acting on each qubit [54]. We can choose the encoding circuit based on this. The number of hidden neurons used to represent hidden variables is fewer than the number of H acting on each qubit. In total, the number of hidden neurons needed is of order $O(N_e + n)$, where N_e is number of edges in the corresponding graph. N_e is at most $O(n^2)$, but we do not usually encounter graph states from dense graphs [55], typically only $O(n \log n)$ or even $O(n)$ hidden neurons are needed. Our representation method is effective and optimal.

Next, we describe topological states with different topological orders within our quantum information frameworks. These topological states encountered can be represented as RBM efficiently.

Fracton topological order.— The Pauli stabilizer formalism covers most of the fracton topological order models [33–35, 38], such as Haah's code [33]. Stabilizers of Haah's code involve two types of stabilizer on eight spins: eight Zs and eight Xs in each cube.

Intrinsic topological order.— We now consider RBM representation for some notable XS stabilizer states: the double semion(an example of string-net model [39]) and many twist quantum double models. We define the double semion model on a honeycomb lattice with one qubit per edge. The wave function of double semion is: $|\psi\rangle = \sum_{x \text{ is loops}} (-1)^{\text{number of loops}} |x\rangle$. In the XS-stabilizer formalism, this model has two types of stabilizer operators: $g_p = \prod_{l\in v} Z_l, g_p = \prod_{l\in p} X_l \prod_{r\in \text{legs of } p} S_r$ corresponding to the vertex s and the face p respectively.

Quantum double models [41] are generalizations of the toric code that describe systems of abelian and non-abelian anyons. Twisted quantum double models are further generalizations of quantum double models [41–43, 56, 57]. Many twisted quantum double models fit into the XS-stabilizer formalism [32], thus can be represented as RBM exactly. Examples include twisted quantum double model $D^{\omega}(\mathbb{Z}_2^n)$ with the group $\mathbb{Z}_2^n$ and different twists $\omega \in H^3(\mathbb{Z}^n, U(1))$ on a triangular lattice, where $H^3(\mathbb{Z}_2^n, U(1))$ is the third cohomology group. The $H^3(\mathbb{Z}_2^1, U(1))$ case includes the double semion. It is known [32, 58] that a non-trivial twist from $H^3(\mathbb{Z}_2^3, U(1))$ harbors non-abelian anyon excitations.

Symmetry protected topological order.— The AKLT model [44, 45] is a one-dimensional spin-1 model with symmetric protected topological order. When we consider the periodic boundary condition, the unique ground state $|\psi_{AKLT}\rangle$, in terms of matrix product state, writes

$$\Psi_{AKLT}(a_1, a_2, \cdots, a_n) \propto \text{Tr}(A_{a_1} A_{a_2} \cdots A_{a_n}), \qquad (5)$$

where $A_{-1} = X$, $A_0 = Y$, $A_{+1} = Z$ and $a_i = -1, 0, +1$. Alternatively, matrix product states can be described as projected entangled pairs states(PEPS) [26]. As shown in Fig. 4, every red line is a EPR pair $|00\rangle + |11\rangle$. Each shaded circle represents a projection from two spins of dimension 2 to a physical degree of dimension 3 (spin-1). $P = \sum_{a_i,\alpha,\beta} A_{a_i,\alpha,\beta} |a_i\rangle\langle\alpha\beta|$ where the summation is over $a_i = -1, 0, 1$ and $\alpha, \beta = 1, 2$. After using unary representation, in the quantum circuit language, the projection P is a map that maps $|01\rangle + |10\rangle \to |010\rangle$, $i(|01\rangle - |10\rangle) \to |001\rangle$ and $|00\rangle - |11\rangle \to |010\rangle$. We find such a quantum circuit made of Clifford gate, as shown in Fig. 4(b). Because all operations lie in Clifford gates, the whole quantum state is a Pauli stabilizer state restricted to the subspace of $|100\rangle, |010\rangle$ and $|001\rangle$. Thus can be represented by RBM with unary hidden neurons(blue neurons in Fig. 1) and other hidden neurons.

We also show RBM can represent other symmetry protected topological order models. These examples include the 2D CZX model (with $\mathbb{Z}_2$ symmetry), and Yoshida's CCZ model [59] (with $\mathbb{Z}_2 \otimes \mathbb{Z}_2 \otimes \mathbb{Z}_2$ symmetry). The

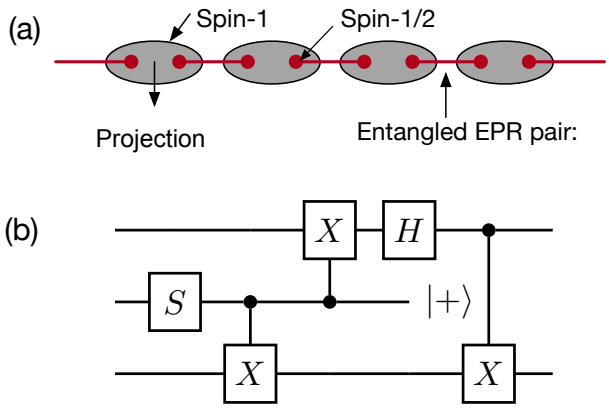

FIG. 4. (a) The ground state of the AKLT model. The spin one on each lattice site can be decomposed into two spin 1/2's which form EPR pairs between nearest neighbor pairs. At the two ends of an open chain, there are two isolated spin 1/2's giving rise to a four-fold ground state degeneracy. Every red line represent a $|00\rangle + |11\rangle$ state. Each shaded circle represent a projection operator $P = |100\rangle(\langle 01| + \langle 01|) + |010\rangle i(\langle 01| - \langle 10|) + |001\rangle(\langle 00| - \langle 11|)$. (b) The Clifford circuit that realizes the projection P under the unary representation(live in the space spanned by $|100\rangle$, $010\rangle$ and $|001\rangle$). Here $|+\rangle$ means projecting onto $|+\rangle$ state.

ground state of the 2D CZX model [46] is a tensor product of GHZ states $|0000\rangle + |1111\rangle$ on each plaquette. Because GHZ state belongs to stabilizer state, RBM can exactly represent the ground state of the 2D CZX model. Similar to SPT cluster state, the ground state of Yoshida's CCZ model [34] on the trivalent lattice is a hypergraph state with 3-hyperedges. Thus it can be represented.

Discussions.— This paper sets out to investigate different topological models with RBM state using tools from quantum information such as the (XS) stabilizer and the (hyper)graph-state formalism. The most significant findings are the fact that RBM state can capture different exotic models within different topological phases: intrinsic topological phase, symmetry protected topological phase and fracton topological phase. It remains open whether RBM can capture additional string-net models such as double Fibonacci. RBM state may be helpful in investigating symmetry enriched topological order [60] and symmetry fractionalization [61] in two-dimensional topological phases. Our exact representation results provide invaluable guidance for future numerical studies on topological phase transitions.

Our results are also of interest to the quantum information community. The Gottesman-Knill theorem [55, 62, 63] states that stabilizer dynamics can be efficiently simulated. Our result which shows RBM states contain stabilizer states suggests classical simulation of an unknown larger family of quantum circuits may benefit from RBM states [24]. Because hypergraph states

allow for an exponentially increasing violation of the Bell inequality [64–67], our results provide analytical evidence for numerical studies [13] on estimating maximum violation of Bell inequality. We leave these for future work. Our method also generalizes to qudit stabilizer states [68] with unary representation.

Acknowledgement.— We thank Dong-Ling Deng, Mingji Xia, and Fan Ye for helpful discussions. This work was supported by Tsinghua University and the National Key Research and Development Program of China (2016YFA0301902).

Note added.— After completion of this work, a preprint appeared in arXiv [71] which gives a different method to represent stabilizer states with the restricted Boltzmann machine.

* gaoxungx@gmail.com
† lmduan@tsinghua.edu.cn

[1] Yann LeCun, Yoshua Bengio, and Geoffrey Hinton. Deep learning. *Nature*, 521(7553):436–444, May 2015.

[2] Ian Goodfellow, Yoshua Bengio, Aaron Courville, and Yoshua Bengio. *Deep learning*, volume 1. MIT press Cambridge, 2016.

[3] Jacob Biamonte, Peter Wittek, Nicola Pancotti, Patrick Rebentrost, Nathan Wiebe, and Seth Lloyd. Quantum machine learning. *Nature*, 549(7671):195–202, September 2017.

[4] Carlo Ciliberto, Mark Herbster, Alessandro Davide Ialongo, Massimiliano Pontil, Andrea Rocchetto, Simone Severini, and Leonard Wossnig. Quantum machine learning: a classical perspective. *Proc. R. Soc. A*, 474(2209): 20170551, 2018.

[5] Ulrich Schollwöck. The density-matrix renormalization group in the age of matrix product states. *Annals of Physics*, 326(1):96–192, 2011.

[6] Frank Verstraete, Valentin Murg, and J Ignacio Cirac. Matrix product states, projected entangled pair states, and variational renormalization group methods for quantum spin systems. *Advances in Physics*, 57(2):143–224, 2008.

[7] Norbert Schuch, Michael M. Wolf, Frank Verstraete, and J. Ignacio Cirac. Simulation of quantum many-body systems with strings of operators and monte carlo tensor contractions. *Phys. Rev. Lett.*, 100: 040501, Jan 2008. doi:10.1103/PhysRevLett.100.040501. URL https://link.aps.org/doi/10.1103/PhysRevLett.100.040501.

[8] David Ceperley and Berni Alder. Quantum monte carlo. *Science*, 231(4738):555–560, 1986.

[9] E. Y. Loh, J. E. Gubernatis, R. T. Scalettar, S. R. White, D. J. Scalapino, and R. L. Sugar. Sign problem in the numerical simulation of many-electron systems. *Phys. Rev. B*, 41:9301–9307, May 1990. doi:10.1103/PhysRevB.41.9301. URL https://link.aps.org/doi/10.1103/PhysRevB.41.9301.

[10] Norbert Schuch, Michael M. Wolf, Frank Verstraete, and J. Ignacio Cirac. Computational complexity of projected entangled pair states. *Phys. Rev. Lett.*, 98: 140506, Apr 2007. doi:10.1103/PhysRevLett.98.140506. URL https://link.aps.org/doi/10.1103/PhysRevLett.98.140506.

[11] F. Verstraete, M. M. Wolf, D. Perez-Garcia, and J. I. Cirac. Criticality, the area law, and the computational power of projected entangled pair states. *Phys. Rev. Lett.*, 96:220601, Jun 2006. doi: 10.1103/PhysRevLett.96.220601. URL https://link.aps.org/doi/10.1103/PhysRevLett.96.220601.

[12] Giuseppe Carleo and Matthias Troyer. Solving the quantum many-body problem with artificial neural networks. *Science*, 355(6325):602–606, 2017. ISSN 0036-8075. doi:10.1126/science.aag2302. URL http://science.sciencemag.org/content/355/6325/602.

[13] Dong-Ling Deng, Xiaopeng Li, and S. Das Sarma. Machine learning topological states. *Phys. Rev. B*, 96: 195145, Nov 2017. doi:10.1103/PhysRevB.96.195145. URL https://link.aps.org/doi/10.1103/PhysRevB.96.195145.

[14] Stephen R Clark. Unifying neural-network quantum states and correlator product states via tensor networks. *Journal of Physics A: Mathematical and Theoretical*, 51 (13):135301, 2018.

[15] Xun Gao and Lu-Ming Duan. Efficient representation of quantum many-body states with deep neural networks. *Nature Communications*, 8(1):662, 2017.

[16] Yichen Huang and Joel E Moore. Neural network representation of tensor network and chiral states. *arXiv preprint arXiv:1701.06246*, 2017.

[17] Dong-Ling Deng, Xiaopeng Li, and S. Das Sarma. Quantum entanglement in neural network states. *Phys. Rev. X*, 7:021021, May 2017. doi:10.1103/PhysRevX.7.021021. URL https://link.aps.org/doi/10.1103/PhysRevX.7.021021.

[18] Zi Cai and Jinguo Liu. Approximating quantum many-body wave functions using artificial neural networks. *Phys. Rev. B*, 97:035116, Jan 2018. doi: 10.1103/PhysRevB.97.035116. URL https://link.aps.org/doi/10.1103/PhysRevB.97.035116.

[19] Jing Chen, Song Cheng, Haidong Xie, Lei Wang, and Tao Xiang. Equivalence of restricted boltzmann machines and tensor network states. *Phys. Rev. B*, 97:085104, Feb 2018. doi:10.1103/PhysRevB.97.085104. URL https://link.aps.org/doi/10.1103/PhysRevB.97.085104.

[20] Ivan Glasser, Nicola Pancotti, Moritz August, Ivan D. Rodriguez, and J. Ignacio Cirac. Neural-network quantum states, string-bond states, and chiral topological states. *Phys. Rev. X*, 8:011006, Jan 2018. doi: 10.1103/PhysRevX.8.011006. URL https://link.aps.org/doi/10.1103/PhysRevX.8.011006.

[21] Zhih-Ahn Jia, Yuan-Hang Zhang, Yu-Chun Wu, Guang-Can Guo, and Guo-Ping Guo. Efficient machine learning representations of surface code with boundaries, defects, domain walls and twists. *arXiv preprint arXiv:1802.03738*, 2018.

[22] Giuseppe Carleo, Yusuke Nomura, and Masatoshi Imada. Constructing exact representations of quantum many-body systems with deep neural networks. *arXiv preprint arXiv:1802.09558*, 2018.

[23] Giacomo Torlai, Guglielmo Mazzola, Juan Carrasquilla, Matthias Troyer, Roger Melko, and Giuseppe Carleo. Neural-network quantum state tomography. *Nature Physics*, 14(5):447–450, 2018.

[24] Bjarni Jónsson, Bela Bauer, and Giuseppe Carleo. Neural-network states for the classical simulation of quantum computing. *arXiv preprint arXiv:1808.05232*, 2018.

[25] Dong-Ling Deng. Machine learning detection of bell nonlocality in quantum many-body systems. *Phys. Rev. Lett.*, 120:240402, Jun 2018. doi: 10.1103/PhysRevLett.120.240402. URL https://link.aps.org/doi/10.1103/PhysRevLett.120.240402.

[26] Bei Zeng, Xie Chen, Duan-Lu Zhou, and Xiao-Gang Wen. Quantum information meets quantum matter–from quantum entanglement to topological phase in many-body systems. *arXiv preprint arXiv:1508.02595*, 2015.

[27] Xiao-Gang Wen. *Quantum field theory of many-body systems: from the origin of sound to an origin of light and electrons*. Oxford University Press on Demand, 2004.

[28] LD Landau and EM Lifshitz. Statistical physics, vol. 5. *Course of theoretical physics*, 30, 1980.

[29] Xie Chen, Zheng-Cheng Gu, Zheng-Xin Liu, and Xiao-Gang Wen. Symmetry-protected topological orders in interacting bosonic systems. *Science*, 338(6114):1604–1606, 2012. ISSN 0036-8075. doi:10.1126/science.1227224. URL http://science.sciencemag.org/content/338/6114/1604.

[30] Ching-Kai Chiu, Jeffrey C. Y. Teo, Andreas P. Schnyder, and Shinsei Ryu. Classification of topological quantum matter with symmetries. *Rev. Mod. Phys.*, 88:035005, Aug 2016. doi:10.1103/RevModPhys.88.035005. URL https://link.aps.org/doi/10.1103/RevModPhys.88.035005.

[31] Daniel Gottesman. Stabilizer codes and quantum error correction. *arXiv preprint quant-ph/9705052*, 1997.

[32] Xiaotong Ni, Oliver Buerschaper, and Maarten Van den Nest. A non-commuting stabilizer formalism. *Journal of Mathematical Physics*, 56(5):052201, 2015.

[33] Jeongwan Haah. Local stabilizer codes in three dimensions without string logical operators. *Phys. Rev. A*, 83:042330, Apr 2011. doi:10.1103/PhysRevA.83.042330. URL https://link.aps.org/doi/10.1103/PhysRevA.83.042330.

[34] Beni Yoshida. Exotic topological order in fractal spin liquids. *Phys. Rev. B*, 88:125122, Sep 2013. doi: 10.1103/PhysRevB.88.125122. URL https://link.aps.org/doi/10.1103/PhysRevB.88.125122.

[35] Han Ma, Ethan Lake, Xie Chen, and Michael Hermele. Fracton topological order via coupled layers. *Phys. Rev. B*, 95:245126, Jun 2017. doi: 10.1103/PhysRevB.95.245126. URL https://link.aps.org/doi/10.1103/PhysRevB.95.245126.

[36] Sagar Vijay, Jeongwan Haah, and Liang Fu. A new kind of topological quantum order: A dimensional hierarchy of quasiparticles built from stationary excitations. *Phys. Rev. B*, 92:235136, Dec 2015. doi: 10.1103/PhysRevB.92.235136. URL https://link.aps.org/doi/10.1103/PhysRevB.92.235136.

[37] Sagar Vijay, Jeongwan Haah, and Liang Fu. Fracton topological order, generalized lattice gauge theory, and duality. *Phys. Rev. B*, 94:235157, Dec 2016. doi: 10.1103/PhysRevB.94.235157. URL https://link.aps.org/doi/10.1103/PhysRevB.94.235157.

[38] Claudio Chamon. Quantum glassiness in strongly correlated clean systems: An example of topological overprotection. *Phys. Rev. Lett.*, 94:040402, Jan 2005. doi: 10.1103/PhysRevLett.94.040402. URL https://link.aps.org/doi/10.1103/PhysRevLett.94.040402.

[39] Michael A. Levin and Xiao-Gang Wen. String-net condensation: A physical mechanism for topological phases. *Phys. Rev. B*, 71:045110, Jan 2005. doi: 10.1103/PhysRevB.71.045110. URL https://link.aps.org/doi/10.1103/PhysRevB.71.045110.

[40] Zheng-Cheng Gu, Michael Levin, Brian Swingle, and Xiao-Gang Wen. Tensor-product representations for string-net condensed states. *Phys. Rev. B*, 79:085118, Feb 2009. doi:10.1103/PhysRevB.79.085118. URL https://link.aps.org/doi/10.1103/PhysRevB.79.085118.

[41] A.Yu. Kitaev. Fault-tolerant quantum computation by anyons. *Annals of Physics*, 303(1):2 – 30, 2003. ISSN 0003-4916. doi:https://doi.org/10.1016/S0003-4916(02)00018-0. URL http://www.sciencedirect.com/science/article/pii/S0003491602000180.

[42] Yuting Hu, Yidun Wan, and Yong-Shi Wu. Twisted quantum double model of topological phases in two dimensions. *Phys. Rev. B*, 87:125114, Mar 2013. doi: 10.1103/PhysRevB.87.125114. URL https://link.aps.org/doi/10.1103/PhysRevB.87.125114.

[43] Salman Beigi, Peter W Shor, and Daniel Whalen. The quantum double model with boundary: condensations and symmetries. *Communications in mathematical physics*, 306(3):663–694, 2011.

[44] Ian Affleck, Tom Kennedy, Elliott H. Lieb, and Hal Tasaki. Rigorous results on valence-bond ground states in antiferromagnets. *Phys. Rev. Lett.*, 59:799–802, Aug 1987. doi:10.1103/PhysRevLett.59.799. URL https://link.aps.org/doi/10.1103/PhysRevLett.59.799.

[45] Ian Affleck, Tom Kennedy, Elliott H Lieb, and Hal Tasaki. Valence bond ground states in isotropic quantum antiferromagnets. In *Condensed matter physics and exactly soluble models*, pages 253–304. Springer, 1988.

[46] Xie Chen, Zheng-Xin Liu, and Xiao-Gang Wen. Two-dimensional symmetry-protected topological orders and their protected gapless edge excitations. *Phys. Rev. B*, 84:235141, Dec 2011. doi:10.1103/PhysRevB.84.235141. URL https://link.aps.org/doi/10.1103/PhysRevB.84.235141.

[47] Marc Hein, Wolfgang Dür, Jens Eisert, Robert Raussendorf, M Nest, and H-J Briegel. Entanglement in graph states and its applications. *arXiv preprint quant-ph/0602096*, 2006.

[48] Matteo Rossi, M Huber, D Bruß, and C Macchiavello. Quantum hypergraph states. *New Journal of Physics*, 15 (11):113022, 2013.

[49] Jeroen Dehaene and Bart De Moor. Clifford group, stabilizer states, and linear and quadratic operations over gf(2). *Phys. Rev. A*, 68:042318, Oct 2003. doi: 10.1103/PhysRevA.68.042318. URL https://link.aps.org/doi/10.1103/PhysRevA.68.042318.

[50] Maarten Van den Nest, Jeroen Dehaene, and Bart De Moor. Graphical description of the action of local Clifford transformations on graph states. *Phys. Rev. A*, 69(2):022316, February 2004.

[51] Markus Grassl, Andreas Klappenecker, and Martin Rotteler. Graphs, quadratic forms, and quantum codes. In *Information Theory, 2002. Proceedings. 2002 IEEE International Symposium on*, page 45. IEEE, 2002.

[52] D Schlingemann. Stabilizer Codes Can Be Realized As

Graph Codes. *Quantum Info. Comput.*, 2(4):307–323, June 2002.

[53] Vaneet Aggarwal and A Robert Calderbank. Boolean functions, projection operators, and quantum error correcting codes. *IEEE Transactions on Information Theory*, 54(4):1700–1707, 2008.

[54] Erik Hostens, Jeroen Dehaene, and Bart De Moor. Stabilizer states and clifford operations for systems of arbitrary dimensions and modular arithmetic. *Phys. Rev. A*, 71:042315, Apr 2005. doi: 10.1103/PhysRevA.71.042315. URL https://link.aps.org/doi/10.1103/PhysRevA.71.042315.

[55] Simon Anders and Hans J Briegel. Fast simulation of stabilizer circuits using a graph-state representation. *Phys. Rev. A*, 73:022334, February 2006.

[56] Alexei Kitaev. Anyons in an exactly solved model and beyond. *Annals of Physics*, 321(1):2–111, 2006.

[57] Oliver Buerschaper. Twisted injectivity in projected entangled pair states and the classification of quantum phases. *Annals of Physics*, 351:447–476, 2014.

[58] Mark de Wild Propitius. (spontaneously broken) abelian chern-simons theories. *Nuclear Physics B*, 489(1-2):297–359, 1997.

[59] Beni Yoshida. Topological phases with generalized global symmetries. *Phys. Rev. B*, 93:155131, Apr 2016. doi: 10.1103/PhysRevB.93.155131. URL https://link.aps.org/doi/10.1103/PhysRevB.93.155131.

[60] Meng Cheng, Zheng-Cheng Gu, Shenghan Jiang, and Yang Qi. Exactly solvable models for symmetry-enriched topological phases. *Phys. Rev. B*, 96:115107, Sep 2017. doi:10.1103/PhysRevB.96.115107. URL https://link.aps.org/doi/10.1103/PhysRevB.96.115107.

[61] Xie Chen. Symmetry fractionalization in two dimensional topological phases. *Reviews in Physics*, 2:3–18, 2017.

[62] Daniel Gottesman. The heisenberg representation of quantum computers. *arXiv preprint quant-ph/9807006*, 1998.

[63] Scott Aaronson and Daniel Gottesman. Improved simulation of stabilizer circuits. *Phys. Rev. A*, 70:052328, November 2004.

[64] Mariami Gachechiladze, Costantino Budroni, and Otfried Guhne. Extreme violation of local realism in quantum hypergraph states. *Phys. Rev. Lett.*, 116: 070401, Feb 2016. doi:10.1103/PhysRevLett.116.070401. URL https://link.aps.org/doi/10.1103/PhysRevLett.116.070401.

[65] Otfried Guhne, Marti Cuquet, Frank ES Steinhoff, Tobias Moroder, Matteo Rossi, Dagmar Bruß, Barbara Kraus, and Chiara Macchiavello. Entanglement and nonclassical properties of hypergraph states. *Journal of Physics A: Mathematical and Theoretical*, 47(33):335303, 2014.

[66] J. S. Bell. On the einstein podolsky rosen paradox. *Physics Physique Fizika*, 1:195–200, Nov 1964. doi:10.1103/PhysicsPhysiqueFizika.1.195. URL https://link.aps.org/doi/10.1103/PhysicsPhysiqueFizika.1.195.

[67] Nicolas Brunner, Daniel Cavalcanti, Stefano Pironio, Valerio Scarani, and Stephanie Wehner. Bell nonlocality. *Rev. Mod. Phys.*, 86:419–478, Apr 2014. doi: 10.1103/RevModPhys.86.419. URL https://link.aps.org/doi/10.1103/RevModPhys.86.419.

[68] Erik Hostens, Jeroen Dehaene, and Bart De Moor. Stabilizer states and clifford operations for systems of arbitrary dimensions and modular arithmetic. *Phys. Rev. A*, 71:042315, Apr 2005. doi: 10.1103/PhysRevA.71.042315. URL https://link.aps.org/doi/10.1103/PhysRevA.71.042315.

[69] Jin-Yi Cai, Pinyan Lu, and Mingji Xia. The complexity of complex weighted boolean# csp. *Journal of Computer and System Sciences*, 80(1):217–236, 2014.

[70] Jin-Yi Cai, Heng Guo, and Tyson Williams. Clifford gates in the holant framework. *Theoretical Computer Science*, 2018.

[71] Yuan-Hang Zhang, Zhih-Ahn Jia, Yu-Chun Wu, and Guang-Can Guo. An efficient algorithmic way to construct boltzmann machine representations for arbitrary stabilizer code. *arXiv preprint arXiv:1809.08631*, 2018.

Detailed derivation of RBM representations of hypergraph states

First we recall the definition of quantum hypergraph state in more detail. Mathematically, hypergraphs are generalization of graphs in which an edge may connect more than two vertices. Formally, a hypergraph H is a pair $H = (X, E)$ where X is a set of element called vertices, and E is a subset of $P(X)$, where $P(X)$ is the power set of X. Given a mathematical hypergraph, the corresponding quantum state can be generated by following similar steps in constructing a graph state: first, assign to each vertex a qubit and initialize each qubit as $|+\rangle$; Then, whenever there is hyperedge, perform a controlled-Z operation between all connected qubits; if the qubits $v_1, v_2, \ldots, v_k$ are connected by a k-hyperedge, then perform $C^k Z_{i_1,i_2,\ldots,i_k}$. As a result, the hypergraph state and its wave function[48] take the form

$$\begin{aligned} |g\rangle &= \prod_{\{i_1,i_2,\ldots,i_k\}\in E} C^k Z_{i_1,i_2,\ldots,i_k} |+\rangle^{\otimes n} \\ \Psi(g) &= \sum_{v_1,v_2,\cdots,v_n} \prod_{\{i_1,i_2,\ldots,i_k\}\in E} (-1)^{i_1 i_2 \ldots i_k} |v_1 v_2 \cdots v_n\rangle. \end{aligned} \tag{6}$$

Next, we give a detailed derivation of realizing correlation factor of the type $(-1)^{v_1 v_2 \cdots v_k}$ using restricted Boltzmann machines. We first recall $(-1)^{v_1 v_2}$ which relates to graph states from [15]:

$$\begin{aligned} H_{v_1,v_2} = \frac{(-1)^{v_1 v_2}}{\sqrt{2}} &= \sum_{h=0,1} e^{W_H(v_1,h)+W_H(v_2,h)} \\ &= \cos\left(\frac{\pi}{4}[2(v_1+v_2)-1]\right). \end{aligned} \tag{7}$$

Note the above equation Eq. 7 is only true for $v_i = 0, 1$. By $\cos v = \frac{1}{2}(e^{iv} + e^{-iv}) = \sum_h e^{iv(2h-1)-\ln 2}$, we have an explicitly formula fo W_H:

$$\begin{aligned} W_H(v_i, h) &= i\pi v_i h - i\pi[2v_i + h]/4 + (i\pi/4 - \ln 2)/2 \\ &= \frac{\pi}{8} i - \frac{\ln 2}{2} - \frac{\pi}{2} iv - \frac{\pi}{4} ih + i\pi vh. \end{aligned}$$

Then we consider $(-1)^{v_1 v_2 v_3}$ with the following decomposition.

$$\begin{aligned} &(-1)^{v_1 v_2 v_3} \\ &= (-1)^{v_1+v_2+v_3} \cdot \left[\frac{8}{3}\cos^2\left(\frac{2\pi}{3}(v_1+v_2+v_3-1)+\frac{\pi}{2}\right)-1\right] \\ &= e^{i\pi(v_1+v_2+v_3)} \cdot \left[\frac{1}{3} + \frac{4}{3}\cos\left[\frac{4\pi}{3}(v_1+v_2+v_3) - \frac{\pi}{3}\right]\right]. \end{aligned}$$

Let $v = \frac{4\pi}{3}(v_1+v_2+v_3) - \frac{\pi}{3}$. The above equation simplifies to

$$\begin{aligned} (-1)^{v_1 v_2 v_3} &= e^{i\pi(v_1+v_2+v_3)} \cdot \left(\frac{1}{3} + \frac{4}{3}\cos v\right) \\ &= e^{i\pi(v_1+v_2+v_3)} \cdot \left(\frac{1}{3} + \frac{2}{3}(e^{iv} + e^{-iv})\right). \end{aligned}$$

The RBM can represent first part by definition. We consider the second part as a RBM with two hidden neurons and set equations:

$$\begin{aligned} \frac{1}{3} + \frac{2}{3}(e^{iv} + e^{-iv}) &= \sum_{h_1,h_2} e^{wvh_1 + w_2 v h_2 + b_1 h_1 + b_2 h_2 + c} \\ &= e^c(1 + e^{w_1 v + b_1} + e^{w_2 v + b_2} + e^{(w_1+w_2)v + b_1 + b_2}). \end{aligned}$$

Solving the above equation, we get $w_1 = -w_2 = \sqrt{-1}$, $b_1 = b_2 = b$, and

$$\begin{aligned} e^c(1 + e^{2b}) &= \frac{1}{3}, \\ e^{b+c} &= \frac{2}{3}. \end{aligned}$$

Solve the above system of equations, we obtain

$$b = \ln(\frac{1 \pm i\sqrt{15}}{4}),$$
$$c = \ln\frac{2}{3} - b.$$

In fact, this construction can be extended to any function of the form $(-1)^{v_1 v_2 \cdots v_k}$. The proof goes as follows. First, we generlize our construction a bit to simulate the correlation factor $2A\cos(\sum_{i=1}^{k} v_i) + B$ by two hidden neurons. Setting the equation:

$$\sum_{h_1,h_2} e^{w_1(\sum_{j=1}^{k} v_j)h_1 + w_2(\sum_{j=1}^{k} v_j)h_2 + b_1 h_1 + b_2 h_2} = A(e^{i(\sum_{i=1}^{k} v_j)} + e^{-i(\sum_{j=1}^{k} v_j)}) + B.$$

Simplifying above equation, we obtain

$$w_1 = -w_2 = i$$
$$e^{c+b_1} = e^{c+b_2} = A,$$
$$e^c(1 + e^{b_1+b_2}) = B.$$

Solving the system of equation, we get

$$b = b_1 = b_2 = \ln(\frac{B \pm \sqrt{B^2 - 4A^2}}{2A}),$$
$$c = \ln A - b = \ln A = \ln\frac{2A^2}{B \pm \sqrt{B^2 - 4A^2}}.$$

Now we proceed to construct RBM representation for $g(v_1, v_2, \cdots, v_k) = (-1)^{v_1 v_2 \cdots v_k}$. Note $g(v_1, v_2, \cdots, v_k)$ equals to 1 only if $v_1 = v_2 = \cdots v_k = 1$, i.e., $v_1 + v_2 + \cdots + v_k = k$.For convenience, we first consider

$$f(\sum_{i=1}^{k} v_i) = \frac{1}{2}(1 - g(\sum_{i=1}^{k} v_i)) = \begin{cases} 1 & v_1 + v_2 + \cdots v_k = k \\ 0 & \text{otherwise} \end{cases}$$

The trick of the construction is to introduce the function

$$t(\sum_{i=1}^{k} v_i) = \cos\left(\frac{2\pi}{k+1}(v_1 + v_2 + \cdots + v_k + 1)\right) = \begin{cases} 1 & v_1 + v_2 + \cdots v_k = k \\ \text{other values} & \text{otherwise} \end{cases}$$

Then the function f can be chosen as (the idea is similar to Lagrange polynomial method)

$$f(\sum_{i=1}^{k} v_i) = \prod_{i=0}^{k} \frac{t(\sum_{i=1}^{k} v_i) - t(i)}{t(i) - t(1)} = \begin{cases} 1 & v_1 + v_2 + \cdots v_k = k \\ 0 & \text{otherwise} \end{cases}$$

Then by substitution we get g

$$g = 1 - 2f = 1 - 2\prod_{i=0}^{k} \frac{t(\sum_{i=1}^{k} v_i) - t(i)}{t(i) - t(1)}$$

In principle we can factorize g into the form of $g(t) = \prod_i (2C_i t + D_i)$, which can then be simulated by RBM term by term.

Derivation details of RBM unary representations

Restricting three neurons only take values from 100, 010 and 001 is equvalently to construct to RBM representation of W state: $|W\rangle = (|001\rangle + |010\rangle + |001\rangle)/\sqrt{3}$. This can be done by two hidden neurons as follow.

Consider the function

$$h(v_1, v_2, v_3) = \begin{cases} 1 & v_1 + v_2 + v_3 = 1 \\ 0 & \text{otherwise} \end{cases}$$

In fact, we find a decomposition of $h(v_1, v_2, v_3)$:

$$h(v_1, v_2, v_3) = (-1)^{v_1+v_2+v_3} \times \left(-\frac{1}{3} + \frac{2}{3} \cos\left(\frac{4\pi}{3}(v_1 + v_2 + v_3) - \frac{\pi}{3} \right) \right),$$

which can be simulated using two hidden neurons using the method from the last section. The weight can be computed.

The notion of W state has been generalized for n qubits to Dicke state. We define $W_{n,k}$ state to be a uniform superposition of all computational basis states $|x\rangle$ where x is a Hamming weight k bit string. This can be done by using nearly the same technique from the last section.

Derivation details on RBM representation of stabilizer state

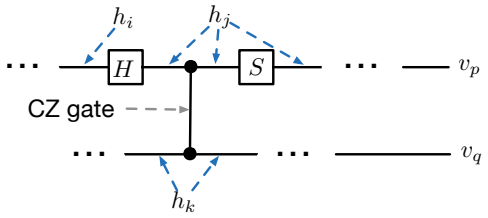

FIG. 5. The close-up of a Clifford circuit. Visible neurons are $v_p, v_q, \cdots$ and hidden neurons are $h_i, h_j, \cdots$. Each H gate corresponds to two neurons with the weight $(-1)^{x_i x_j}$; Each S gates corresponds to one neuron with the weight i^{x_j}; Each CZ gate corresponds to two neurons with the weight $(-1)^{x_1 x_2}$. The whole wave function is a DBM which can be eliminated to a RBM.

The wave function can be represented by a DBM as follow. We denote visible neurons as $v_p, v_q, \cdots$ and hidden neurons as $h_i, h_j, h_k \cdots$. For convenience. We unify the notation of these neurons as $x_i, x_j, x_k, \cdots$ here. As shown in Fig. 5: each H gate corresponds to two neurons with the weight $(-1)^{x_i x_j}$; each S gates corresponds to one neuron with the weight i^{x_j} (even though each single qubit matrix has two indices); each CZ gate corresponds to two neurons with the weight $(-1)^{x_1 x_2}$. Multiplying together and sum over all the hidden indices, we can get the wave function of the stabilizer state:

$$\Psi(v_p, v_q, \cdots) \propto \sum_{h_i, h_j, \cdots} i^{L(h_i, h_j, \cdots, v_p, v_q, \cdots)} (-1)^{Q(h_i, h_j \cdots, v_p, v_q, \cdots)}, \tag{8}$$

where L and Q are affine (with linear and constant terms) and quadratic (without linear term) polynomials with integer coefficients.

Next, we reduce this DBM to a RBM with the following strategy: after eliminating a h_i for some i, the remaining term still keeps the form shown in Eq. 8 except an additional parity constraint on some of $v_p, v_q, \cdots$. Here, we consider the effect of eliminating h_i in detail:

(1) If the coefficient of h_i in L is 0 or 2, ignoring the terms not depending on h_i, the remaining in Eq. 8 could be written as:

$$\sum_{h_i} (-1)^{h_i L'_i} = 2\delta(L_i^p \mod 2)$$

where δ means constraint and L_i^p is an affine polynomial involves those x_j which interact with h_i in Q and constant terms which are the coefficients of h_i in L. There are two cases for L_i^p:

(1.1) If L_i^p only involves visible neurons, we can put this constraint δ before the summation in Eq. 8;
(1.2) If L_i^p involves hidden neurons, e.g. h_j, then we can solve the equation $L_i^p = 0 \mod 2$ by $h_j = L_i^{p\prime} \mod 2$. After the summation of h_j, the only remaining terms are those satisfying $h_j = L_i^{p\prime} \mod 2$ so we can replace h_j by $L_i^{p\prime}$ in Q and by $(L^{p\prime})^2$ in L (because $L^{p\prime} \mod 2 = (L^{p\prime})^2 \mod 4$) in Eq. 8. The key point is: the coefficients of quadratic terms in $(L^{p\prime})^2$ are always 2 thus they keeps the same form as the terms in the summation of Eq. 8 after summation over h_i and h_j.

(2) If the coefficient of h_i in L is 1 (the case for 3 is similar), ignoring the terms not depending on h_i, the remaining in Eq. 8 can be written as:

$$\sum_{h_i} (-1)^{h_i L_i^p} i^{h_i} = (1+i) i^{3(L_i^p)^2}$$

The key point is that the coefficient of quadratic terms in $(L_i^p)^2$ is 2 thus it keeps the same form as the terms in the summation of Eq. 8 after summation over h_i

After eliminating all the hidden variables, the wave function could be written as the form of Eq. 3. The parity constraints could be represented by a hidden neuron with the corresponding visible neurons as shown before.